Arch. Metall. Mater. **64** (2019), 4, 1263-1268

DOI: 10.24425/amm.2019.130089

T. SADOWSKI*#, M. NOWICKI*, P. GOLEWSKI*

THE INFLUENCE OF THE USE OF FASTENERS WITH DIFFERENT STIFFNESS IN HYBRID JOINTS SUBJECTED TO COMPLEX MECHANICAL LOADS

To this day, most of the papers related to hybrid joints were focused on single and double lap joints in which shear deformation and degradation was the dominant phenomenon. However, in real constructions, complex state of loads can be created by: a) torsion with shear, b) bending with shear, c) torsion with tensile.

Analytical and numerical computation for simple mechanical joints is known, however, the introduction of an adhesive layer to this joint makes the load transferred both through: (1) the adhesive and (2) mechanical fasteners. There is also an interaction between the amount and stiffness of mechanical fasteners and the strength of the adhesive layer.

The paper presents the results of numerical calculations for the bending with shear type of load for the hybrid structural joint and corresponding simple joints by: (1) pure adhesion and (2) rivets with different quantity maintaining the same cross-sectional area. A total of 9 simulations were performed for: (1) 4 types of pure rivets connections, (2) pure adhesive joint and (3) 4 kinds of hybrid joints. The surface-based cohesive behavior was used for creation of the adhesive layer, whereas the rivets were modelled by connector type fasteners, which simplify complexity of the numerical model. The use of connectors allowed for effort assessment taking into account damage in both types of connections. Application of connector elements can be useful for larger structures modelling, e.g. aircraft fuselage, where the number of mechanical joints is significant and complex load conditions occur.

Keywords: hybrid joining, fasteners, adhesive, mechanical loads, numerical modelling

1. Introduction

In the last century there was a rapid increase in discoveries and applications in the field of synthetic adhesive joints. The first commercial synthetic adhesive was produced in 1920, their development continues to this day. The reasons for continuous research are: complex mechanisms occurring in the joint and the influence of various parameters, e.g.: defects [1], temperature [2], stiffness of joined materials [3-4], complex stress states [5-6]. Also mechanical connections have been used for many years in construction (steel halls, bridges), machine building, aircrafts and the automotive industry. Among the mechanical connections, we can distinguish: riveted connections [8-10], welded [19], spot welded [12-13,20], clinched [14-15,24], using screws [23,25], shaped [16-17] and friction welded [18,21-22].

Most of these connections have a common feature – they are spot connections. Therefore, in order to reduce stress concentration, their hybrids, e.g. adhesive-rivet connections [7,11-12], are also used. In many cases, such joints are subjected to complex states of stress, which makes it difficult or impossible to formulate the mathematical description of the connection response. In addition, adhesive joints are sensitive to many of technological parameters, e.g. the method of surface preparation or chamfering the ends of flaps [8,10]. Therefore, laboratory tests and numerical analysis are still carried out in this area. They very often concern the issues of joining steel profiles with a composite part in application to shipbuilding [25,27,28].

Paper [25] presents a comparison of connection made of adhesive and mechanical connector with the "co-infused perforated". For the 4-point bending, the second type of connection was stronger, but the differences are on the order of a few percent. In [27], 14 different configurations of metal-composite connections subjected to bending were considered. To maintain a flat surface at the overlap joint, the composite part must be shaped accordingly. By using a double overlap and foam increasing stiffness, one can get an increase of the joint capacity by 44% in relation to the reference model. In [28], laboratory tests were carried out for joining with various screw diameters. Numerical studies were carried out for the model using shell elements (general model) and detailed for plane stress.

Mechanical connections are also used in structures subjected to complex loads (bending and twisting), e.g. in the frame of the car structure [26]. By using a composite connector consisting of two halves, the welding process was eliminated.

When conducting numerical calculations, the way of reflecting of connection work is also important.

The exact 3D model of the overlap connection using a mechanical connector is shown in [29]. The authors point out that

* LUBLIN UNIVERSITY OF TECHNOLOGY, DEPARTMENT OF SOLID MECHANICS, 40 NADBYSTRZYCKA STR., 20-618 LUBLIN, POLAND

Corresponding author: sadowski.t@gmail.com

the use of a 3D element is not appropriate for large structures that include multiple connections. That is why simplifications in the form of fastener are necessary. The elastic-plastic model with damage was used to describe the connector. However, the effect of distribution of mechanical connectors has not been studied.

Two types of arrangement of mechanical connectors were considered in [30]. They concerned the connection of a sandwich type with a steel sheet. It is a complicated connection due to a large change in thickness, therefore two tests were carried out: uniaxial compression and 3-point bending. However, no adhesive layer was included in the joint.

Torsion is also an important load. The authors of work [31] investigated its impact on the connection of two section pipes made of: composite and steel. An adhesive connection occurred between them. The residual stresses in the composite structure created during the curing of the prepreg were taken into account. There was no mechanical connection.

In summary, at present there are many papers for hybrid connections, operating in simple or complex load states, but in most cases they are solutions to a specific engineering problems.

The present paper shows more general solutions concerning the influence of the amount and distribution of mechanical fasteners in a hybrid connection subjected to a complex load condition, i.e. bending with shear. The important parameter in the proposed approach was the constant cross-sectional area of all mechanical fasteners in each simulation. This type of analysis can help in the development of a mathematical description of the work of hybrid joints and also allows engineers to design properly this type of connections.

The aim of this work was to describe the influence of the arrangement of mechanical fasteners, with the same total surface of cross-section, on the strength parameters of the joint. This effect was demonstrated in the rivet and hybrid rivet-adhesive joints.

2. Numerical model

The numerical model was made and calculated in the Abaqus Explicite.

2.1. Adhesive layer model

The adhesive layer model with damage (for Hysol loctite 9514) was created as the surface-based cohesive behavior, similar to [11,32]. Adhesive parameters necessary to modelling were collected in Table 1. To describe damage initiation in the adhesive layer, the maximum stress criterion was used:

$$MAX\left\{\frac{\langle t_n\rangle}{t_n^{\max}}, \frac{t_s}{t_s^{\max}}, \frac{t_t}{t_t^{\max}}\right\} = 1 \tag{1}$$

whereas propagation of cracks was described by the fracture energy parameter G_c [11,32], assessed in [33].

TABLE 1

Value of strength parameters for adhesive layer used in the model

Kind of parameter of adhesive	Hysol loctite 9514
Density [kg/m^3]	1440
Young modulus [GPa]	1.46
Tensile strength [MPa]	44
Shear strength [MPa]	45
Fracture energy G_c [J/m^2]	905

2.2. Elasto-plastic models with damage of mechanical fasteners and joined sheets

The details of mechanical fasteners model with damage process are presented in [32]. It is simplification of the "connector" type of joint included in Abaqus programme with application of constitutive law for its behavior under tension and shear estimated in own experiments, [32]. Strength parameters of applied mechanical connectors were collected in Table 2.

The metallic sheets were modeled as elastic-plastic aluminum material with continuous damage process (e.g. [32-44]). The yield stress for analysed aluminium is equal to $\sigma_y = 470$ MPa, whereas the maximum stress value is reached for $\sigma_{max} = 652$ MPa

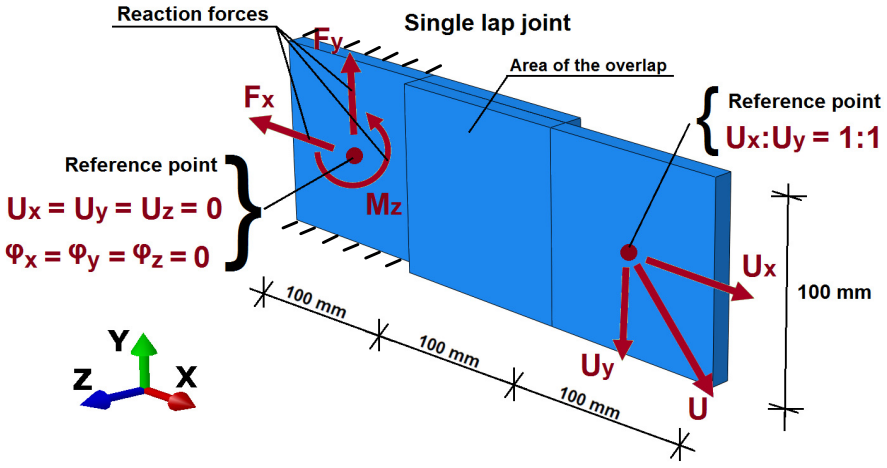

Fig. 1. Numerical model of single lap joins, made of two plates 200 × 100 × 20 mm each

TABLE 2

Value of strength parameters for single rivet used in all models

Kind of model	Axial tensile strenght		Shear strenght	
	Plastic force [N]	Max force [N]	Plastic force [N]	Max force [N]
Model with 2 rivets	4029.6	9600	4004	16800
Model with 4 rivets	2014.8	4800	2002	8400
Model with 8 rivets	1007.4	2400	1001	4200
Model with 16 rivets	503.7	1200	500.5	2100

2.3. Geometries and boundary conditions of the analysed joints

The joined sheets shown in Fig. 1 were subjected to a complex load condition introduced by 2 dimensional displacement components U_x and U_y ($U_x = U_y$). The joint is fixed to the stiff wall in the whole bonding area (left area – 100 mm × 100 mm) by removing of all degrees of freedom. The all resultant reactions F_x, F_y and M_z for this kind of support were focused in one "reference point".

In this study, a total of 9 cases with different combinations of connections in the overlap area were analyzed:

- Case 1 – joining by mechanical connectors (4 models) in quantities of 2, 4, 8, 16 pcs. (Fig. 2). The characteristic feature in all joints types is the same total shear strength of connectors equal to 33.6 kN, and the same tensile strength equal to 8,008 kN.
- Case 2 – connection by pure adhesive layer (1 model).
- Case 3 – hybrid connections obtained by combination of mechanical fasteners (Fig. 2) and adhesive layer.

3. Numerical results

3.1. Case 1 – joining by mechanical connectors

In the first connection case, 4 load simulations were carried out with different number and distribution of rivets shown in Fig. 2. The calculations were carried out until the connection was completely destroyed. Due to the fact that the displacement U is composed of two components U_x and U_y, reactions in the support area can be presented as the resultant force F, F_x, F_y, and M_z, related to U or U_x and U_y, Fig. 3, Fig. 4.

In Fig. 3a distributions of the resultant force F as a function of displacement U for different quantities of mechanical connectors were shown. Here it can be seen similar values of maximum forces for all cases. Their distributions are also very close. Only for the case with 2 rivets one can observe much less stiffness in comparison to the rest of cases. The characteristic feature is gradual increase in stiffness of the joints with the increase of the connectors number. A comparable character of the force distribution to the previous case is shown by the $F_x - U_x$ correlation, Fig. 3b. The maximum value is about 93% of the resultant force F.

A quite different shape one can notice for the component F_y (Fig. 4a) and the associated bending moment M_z (Fig. 4b). The first one is significantly smaller in comparison to the resultant forces F – approximately at the level of 6 - 8%. A characteristic feature of the forces F_y and moments M_z is that they change the sign (due to damage of upper fasteners) along with the increasing displacement U and only then fall to zero.

Energy absorption E_a, calculated as an area under the force-displacement diagram, in all cases is included in Table 4. The case with 2 rivets has the highest value of E_a equal to 31.8 J. This parameter in the rest of cases is equal: 28.8 J (4 rivets), 26.5 J (8 rivets), 25.2 J (16 rivets).

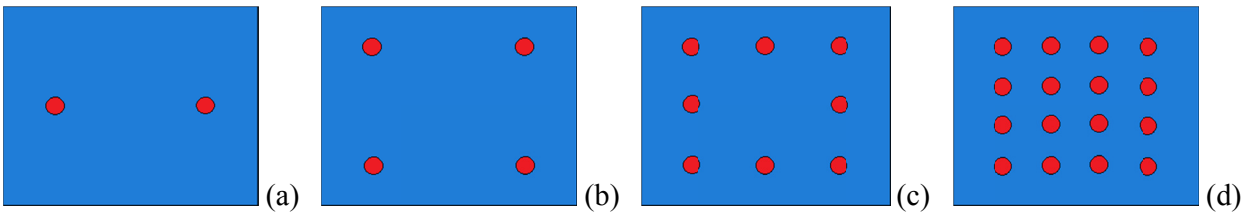

Fig. 2. Distribution of mechanical fasteners on the surface of the overlap 10 × 10 cm: (a) 2 rivets; (b) 4 rivets; (c) 8 rivets; (d) 16 rivets

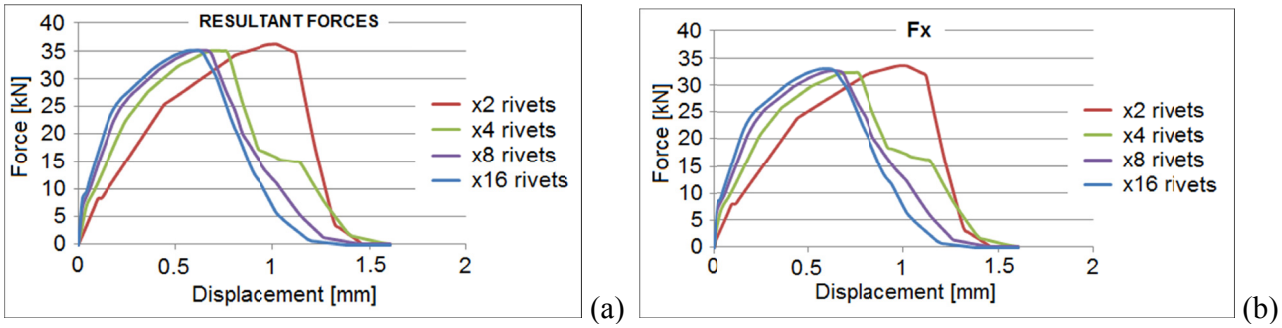

Fig. 3. Force-displacement diagrams for mechanical connection by rivets: (a) resultant forces F vs. U; (b) force F_x vs. U_x

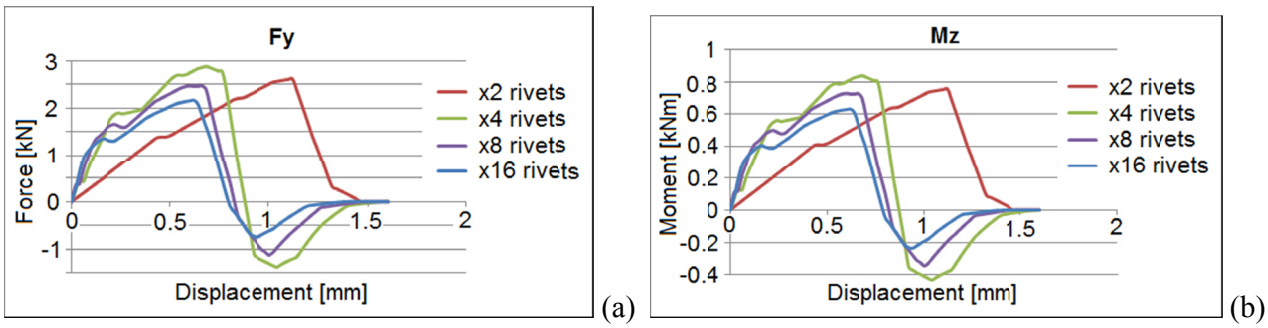

Fig. 4. Force-displacement diagrams for mechanical connection by rivets: (a) force F_y vs. U_y, (b) moment component M_z vs. U_x

3.2. Case 2 – pure adhesive joint

The second case discussed is the pure adhesive connection. This simulation was performed to analyze the load capacity of the joint without mechanical connectors and to compare it with corresponding forces for all types of hybrid connections. Figures 5 and 6 show distributions of the resultant force F and its components F_x, F_y as well as the bending moment M_z for all different types of joints. Both graphs show the effect of the adhesive layer influence on the strength and load capacity for chosen representative connection with 4 rivets.

In Fig. 5 one can notice visible increase of the stiffness in the adhesive joint compared to the riveted one. The pure adhesive connection has also much higher strength than the purely mechanical one obtained by riveting. On the other hand, the maximum value of the resultant force F and F_y component in case of the hybrid connection is not significantly much higher than the purely adhesive connection (by approx. 10%).

For the force component F_y and the moment M_z (Fig. 6) we observed completely different shapes in comparison to the resultant forces F and F_x. The values of these forces and moments are very small in relation to the resultant force F and their distributions are different. The initial stiffnesses in y direction are similar in every type of connection. The highest values of the carrying force occurred for riveted connections.

In case of the joint with adhesive layer the value of energy absorption E_a is the smallest and equal to 21.1 J (Table 4).

3.3. Case 3 – hybryd joint by mechanical connectors and the adhesive layer.

The last case is rivet-adhesive hybrid joint with different amounts of rivets (Fig. 2). In total, 4 simulations were performed here for each number of rivets, see Fig. 2. This analysis was performed to show the influence of: (1) the amount and (2)

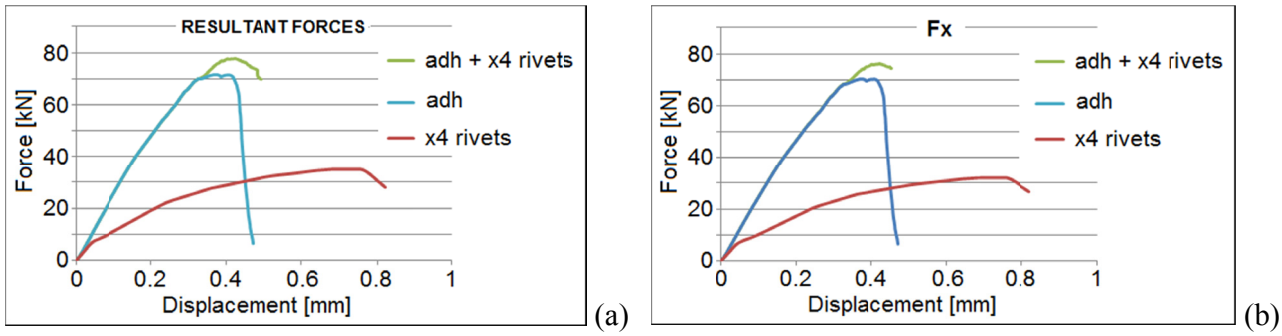

Fig. 5. Comparative force-displacement diagrams for different type of joints: (a) resultant forces F vs. U; (b) force F_x vs. U_x

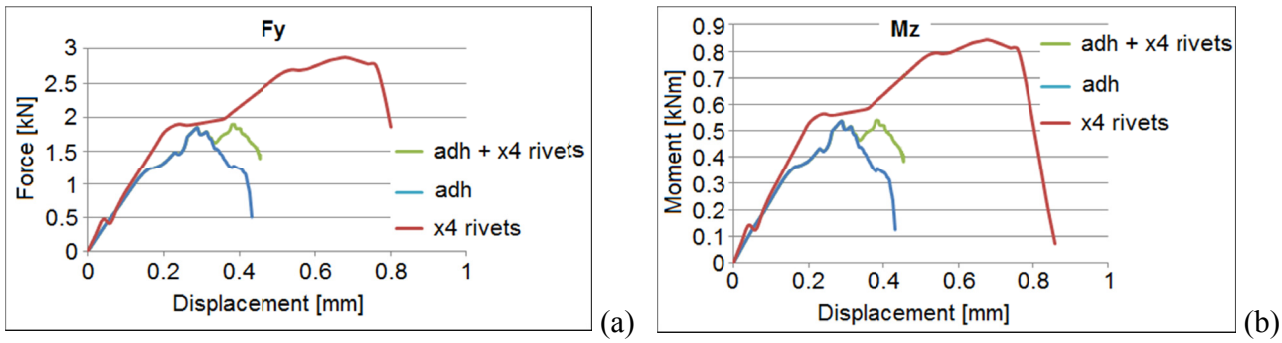

Fig. 6. Comparative force-displacement diagram for different type of joints: (a) force F_y vs. U_y, (b) moment component M_z vs. U_x

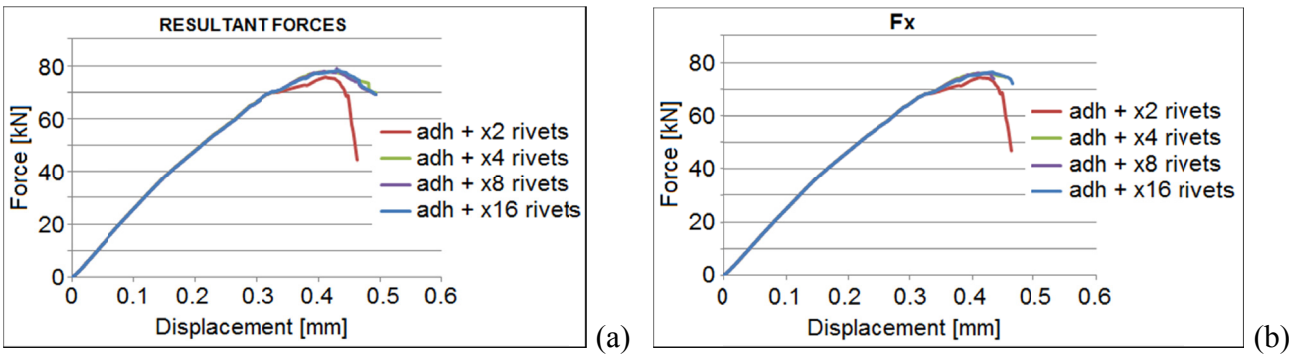

Fig. 7. Force-displacement diagram for hybrid joints by adhesive and different number of rivets: (a) resultant forces F vs. U; (b) force F_x vs. U_x

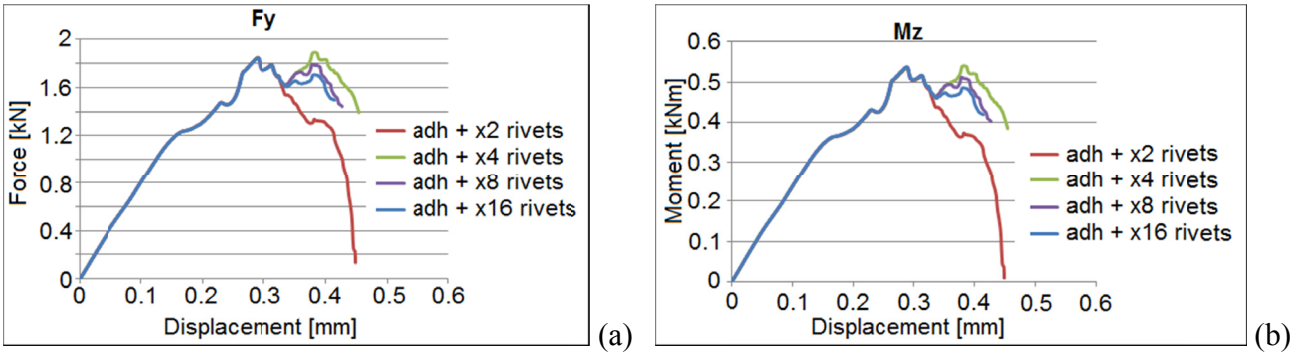

Fig. 8. Force-displacement diagram for hybrid joints by adhesive and different number of rivets: (a) force F_y vs. U_y, (b) moment component M_z vs. U_x

distribution of rivets in the hybrid joints. As it was shown in section 3.2, the initial stiffnesses of such joints are the same as for pure adhesive ones. In Figs 7 and 8 it can also be seen that the number of connectors in hybrid combinations does not affect their stiffness significantly. Values of the maximum forces F have also approximately the similar level in each case. Only for the joint with 2 rivets one can notice slight deviations.

The component F_x is about 98% of the resultant force F, while the component F_y is almost negligible and equal to only 2%.

Table 3 shows values of the resultant forces F [kN] with the displacement U_{max} = 0.4 mm for all analyzed joints.

TABLE 3

Value of resultant forces F [kN] with a displacement of 0,4 mm

Type of connection	Number of connectors [pcs]			
	2	4	8	16
Mechanical connectors	21.90	26.78	29.13	30.35
Adhesive layer	70.21			
Hybryd connection	73.77	75.73	75.61	75.25

The hybrid joints have a slightly higher energy absorption E_a in comparison to the pure adhesive joint (Table 4). However, these values of E_a are smaller in relation to the mechanical connectors joints. The minimum of the E_a is in case of the joint with 2 rivets, i.e. 23.7 J. For 4, 8 and 16 rivets the E_a have almost the same values equal to 25 J, Table 4.

TABLE 4

Value of energy absorption E_a [J]

Type of connection	Number of connectors [pcs]			
	2	4	8	16
Mechanical connectors (rivets)	31.8	28.8	26.49	25.24
Adhesive layer	21.1			
Hybrid joints	23.65	25.11	24.96	24.97

4. Summary

The paper presents results of numerical simulations of deformation processes and estimation of load capacities of hybrid rivet-adhesive joints created with different numbers of mechanical fasteners. The analysis showed the influence of different numbers of mechanical connectors, having the same cross sections, on the load capacity (maximum of the resultant force F) and deformability (force-displacement diagrams) of all types of joints including also the purely adhesive and the purely mechanical ones.

The basic conclusions that result from the presented analyses for purely riveted joints (1st case) are the following:

- the values of resultant forces F for all rivets configurations are almost the same,
- the main component of the resultant force is F_x – around 93%,
- the increase of the number of rivets causes a gradual growth of the stiffness joints,

- the component F_y and the associated moment M_z are relatively small and change the values before total failure of the joints,
- the smaller number of rivets results in increase of the force component F_y values.

Conclusions resulting from the analysis of the pure adhesive joint (2nd case) are the following:

- the adhesive joint has much higher stiffness in comparison to the riveted joints and approximately the same stiffness as the hybrid connection,
- the adhesive layer increases the value of the maximum resultant force F,
- the value of the component F_y is much higher in the riveted joints. The same applies to the moment M_z.

Conclusions resulting from analysis of the hybrid joints (3th case) are the following:

- the stiffness and the maximum force F_{max} do not change significantly with the increase of mechanical fasteners number,
- the component F_x is about 98% of the resultant force F, and the component F_y is almost negligible (only 2%).

Acknowledgement

This work was financially supported by Ministry of Science and Higher Education (Poland) within the statutory research number S/20/2019.

REFERENCES

[1] E.F. Karachalios, R.D. Adams, L.F.M. da Silva, Int. Jour. of Adh. & Adh. **45**, 69-76 (2013).
[2] L.D.R. Grant, R.D. Adams, L.F.M. da Silva, Int. Jour. of Adh. & Adh. **29**, 535-542 (2009).
[3] E.F. Karachalios, R.D. Adams, L.F.M. da Silva, Int. Jour. of Adh. & Adh. **43**, 81-95 (2013).
[4] E.F. Karachalios, R.D. Adams, L.F.M. da Silva, Int. Jour. of Adh. & Adh. **43**, 96-108 (2013).
[5] E.F. Karachalios, R.D. Adams, L.F.M. da Silva, Jour. of Adh. Sci. and Tech. **27**, 1811-1827 (2013).
[6] F. Moroni, A. Pirondi, C. Pernechele, A. Gaita, L. Vescovi, Frac. and Struc. Int. **47**, 294-302 (2019).
[7] F. Moroni and A. Pirondi, Adv. Struct. Mat. **6**, 79-108 (2011).
[8] T. Sadowski, P. Golewski, Key Eng. Mater. **607**, 49-54 (2014).
[9] T. Sadowski, P. Golewski, Arch. of Metall. and Mater. **58**, 581-587 (2013).
[10] P. Golewski, T. Sadowski, Int. Jour. of Adh. and Adh. **77**, 174-182 (2017).
[11] T. Sadowski, M. Nowicki, D. Pietras, P. Golewski. Inter. Jour. of Adh. and Adh., **89**, 72-81 (2019).
[12] T. Sadowski, P. Golewski, M. Kneć, Comp. Struc. **112**, 66-77 (2014).
[13] T. Sadowski, M. Kneć, P. Golewski, (2014) Key Eng. Mater. **601**, 25-28 (2014).
[14] T. Balawender, T. Sadowski, P. Golewski, Comp. Mat. Sc. **64**, 270-272 (2012).
[15] T. Sadowski, T. Balawender, Adv. Struct. Mat. **6**, 149-176 (2011).
[16] T. Sadowski, P. Golewski, V. Radoiu, Solid State Phen. **254**, 1-7 (2016).
[17] P. Golewski, T. Sadowski, IOP Conf. Ser.: Mater. Sci. Eng. **416**, 1-6 (2018).
[18] P. Lacki, A. Derlatka, Comp. Struct. **159**, 491-497 (2017).
[19] P. Lacki, K. Adamus, Comp. and Struc. **89**, 977-985 (2011).
[20] P. Lacki, J. Niemiro, Comp. Struc. **159**, 538-547 (2017).
[21] K. Adamus, J. Adamus, J. Lacki, Comp. Struc. **202**, 95-101 (2018).
[22] P. Lacki, A. Derlatka, Comp. Struc. **202**, 201-209 (2018).
[23] P. Lacki, J. Nawrot, A. Derlatka, J. Winowiecka, Comp. Struc. **211**, 244-253 (2019).
[24] T. Balawender, Acta Metall. Slov. **24**, 1, 58-64 (2018).
[25] J. Cao, J.L. Grenestedt, Comp. Part A **35**, 1091-1105 (2004).
[26] M.P. Cavatorta, D.S. Paolino, L. Peroni, M. Rodino, Comp. Part A **38**, 1251-1261 (2007).
[27] J.P. Kabche, V. Caccese, K.A. Berube, R. Bragg, Comp. Part B **38**, 66-78 (2007).
[28] V. Caccese, J.P. Kabche, K.A. Berube, Comp. Struct. **81**, 450-462 (2007).
[29] Z. Kapidzic, L. Nilsson, H. Ansell, Comp. Struct. **109**, 198-210 (2014).
[30] K. Zhang, D. Shi, W. Wang, Q. Wang, Comp. Struct. **160**, 1198-1204 (2017).
[31] J.H. Oh, Comp. Sci. and Tech. **67**, 1340-1347 (2007).
[32] T. Sadowski, M. Nowicki. IOP Conf. Ser.: Mater. Sci. Eng. **416**, 1-7 (2018).
[33] A. Pirondi, D. Fersini, E. Perotti, F. Moroni. Atti del Congresso IGF, **19**, 85-93 (2007).
[34] T. Sadowski, L. Marsavina, Comput. Mater. Sci. **50**, 1336-1346 (2011).
[35] T. Sadowski, Comput. Mater. Sci. **64**, 209-211 (2012).
[36] V. Burlayenko, H. Altenbach, T. Sadowski, S.D. Dimitrova, Comput. Mater. Sci. **116**, 11-21 (2016).
[37] T. Sadowski, L. Marsavina, N. Peride, E.M. Craciun, Comput. Mat. Sci. **46**, 687-693 (2009).
[38] T. Sadowski, J. Bęc, Comput. Mat. Sci. 50, 1269-1275 (2011).
[39] H. Dębski, T. Sadowski, Comput. Mater. Sci. **83**, 403-411 (2014).
[40] J. Gajewski, T. Sadowski, Comput. Mat. Sci. **82**, 114-117 (2014).
[41] M. Birsan, T. Sadowski, L. Marsavina, D. Pietras, Int. J. Solids Struct. **50**, 519-530 (2013).
[42] G. Golewski, T. Sadowski, Const & Build. Mat. **51**, 207-214 (2014).
[43] T. Sadowski, Mech. Mat. **18**, 1-16 (1994).
[44] V. Burlayenko, T. Sadowski, Comput. Mat. Sci. **52**, 212-216 (2012).